Energy dependent transport length scales in strongly diffusive carbon nanotubes

2006 J. Phys.: Condens. Matter 18 4581

(http://iopscience.iop.org/0953-8984/18/19/012)

INSTITUTE OF PHYSICS PUBLISHING JOURNAL OF PHYSICS: CONDENSED MATTER

J. Phys.: Condens. Matter **18** (2006) 4581–4587 doi:10.1088/0953-8984/18/19/012

Energy dependent transport length scales in strongly diffusive carbon nanotubes

B Lassagne[1], B Raquet[1], J M Broto[1] and J González[2]

[1] Laboratoire National des Champs Magnetiques Pulsés, UMR5147 143 avenida de rangueil, 31400 Toulouse, France
[2] Centro de Estudios de Semiconductores Facultad de Ciencias, Departamento de Física, Universidad de Los Andes, Mérida, Venezuela

Received 20 October 2005, in final form 21 October 2005
Published 26 April 2006
Online at stacks.iop.org/JPhysCM/18/4581

Abstract

We report magneto-transport measurements in parallel magnetic field and μ-Raman spectroscopy on diffusive multiwall carbon nanotubes. The disorder effects on the characteristic transport lengths are probed by combining applied magnetic field and back-gate tuning of the Fermi level. Modulations of the differential conductance versus energy depict the modulation of the strength of the weak localization. Both the electronic mean free path and the phase coherence length are found to be energy dependent. The role of disorder in the density of states and in the characteristic transport lengths is discussed.

1. Introduction

The basic understanding of the remarkable electronic properties of carbon nanotubes (CNTs) is currently under intense study. In recent years, transport experiments on individual CNTs gave evidence of several very distinct conduction regimes. Single wall carbon nanotubes are found to act as ballistic electron waveguides with Fabry–Perot interference [1], Luttinger liquids (LLs) [2], quantum dots at lower temperature [3] or one-dimensional diffusive conductors [4]. For multi-wall carbon nanotubes (MWCNTs) as well, a few studies reveal a ballistic behaviour at room temperature [5] while others demonstrate the existence of zero bias anomaly [6] or quantum corrections to the conductivity like weak localization (WL) typical for diffusive systems [7–9]. Deviations from the expected 1D conduction of a pristine tube are somehow connected to native defects which affect the electronic transport in a complex way. The electronic backscattering probability depends on the spatial extension of the disorder potential [10], its atomic nature [11] and the Fermi level location (E_F).

Theoretical works emphasize the role of defects in the electronic band structure and the diffusion coefficient. With homogenous disorder (Anderson-like disorder) [12] and a non-energy-dependent phase coherence length (L_φ), enhancement of the electronic scattering resulting from increased available energy states appears at the onset of the van Hove singularities (vHSs). It induces an electronic mean free path (l_e) strongly dependent on E_F.

Other studies based on the density functional calculation on a perfect nanotube point out a drastic modification of the band structure along with a drop of conductivity due to resonant scattering on localized states originating from *one* defect like a vacancy or impurity [11]. A combination of the two models [13] shows that by chemically changing the electronic doping of the tube the conduction goes from ballistic to quantum interference in the weak localization regime.

Using recent linear resistance measurements with a metallic AFM tip, Gomez-Navarro *et al* [14] established that by controlling the defect density by ion irradiation the conductance of single wall nanotubes can be tuned in the Anderson localization regime. On the other hand, evidence of disorder effects on the band structure requires conductivity measurements with a gate voltage tuning of E_F. Several works reveal complex conductance modulations versus gate voltage ($G(V_g)$), on which the disorder effect is hard to extract [9, 15, 16]. Charge effects, universal conductance fluctuations (UCFs) and band-structure characteristics also contribute to $G(V_g)$. One way to discriminate is to combine the scanning of E_F with temperature dependence and magneto-transport conductance measurements under high magnetic field parallel to the tube axis [17]. Direct measurements of field-induced quantum phenomena like quantum interference effects in the WL regime or Aharonov–Bohm oscillation (AB) in the ballistic or semi-ballistic CNTs unveil the conduction regime [18] and the energy-dependent disorder contribution.

In a recent paper [19], we focused on double wall carbon nanotubes and the interplay of WL and AB depending on the electrostatic doping in the vicinity of the charge neutrality point (CNP). Here, we present results on larger MWCNTs in a strong diffusive regime. Structures on the differential conductivity curves as a function of E_F are assigned to disorder. Combined with 30 T magneto-transport experiments, we give experimental evidence of the strong dependence of characteristic transport lengths (both l_e and L_φ) on energy in the presence of disorder.

2. Experimental results and analysis

2.1. Electronic characterization

We perform experiments on MWCNTs from Nanocyl and produced by chemical vapour deposition techniques (CVD). Tubes are deposited on Si/SiO_2 (100 nm) substrates and thermally evaporated Pd electrodes are used to make top contacts on individual tubes [17]. Results presented here are obtained on a 10 nm diameter MWCNT (AFM estimate) with 250 nm length between contacts.

Electronic measurements are performed in a two probe configuration between 300 and 2 K, using the Si substrate as a back gate and a 35 T pulsed magnetic field parallel to the tube axis. Between 300 and 70 K, the resistance slightly increases from 150 to 180 kΩ with linear $I(V)$ curves.

Below 70 K, one observes a power law dependence of the conductance versus temperature $G(T)$ (figure 1). At 4 K, resistance ranges between 500 kΩ and 1.5 MΩ according to the gate voltage between ±6 V and no pronounced zero bias anomaly is observed. The absence of any thermally activated regime (which will be proved hereafter) on $G(T)$ down to 2 K rules out Coulomb blockade and semiconductor behaviour. We conclude therefore that we measure a metallic nanotube in the diffusive regime with Ohmic contacts with Pd electrodes [16].

Details on the differential conductance versus V_g at low temperatures reveal interesting structures with two kinds of modulations (figure 2): fast and non-periodic oscillations superimposed on slow modulations with large minima around ±2 V. Usually, fast and non-periodic oscillations in mesoscopic systems can be attributed to UCF. A large L_φ results

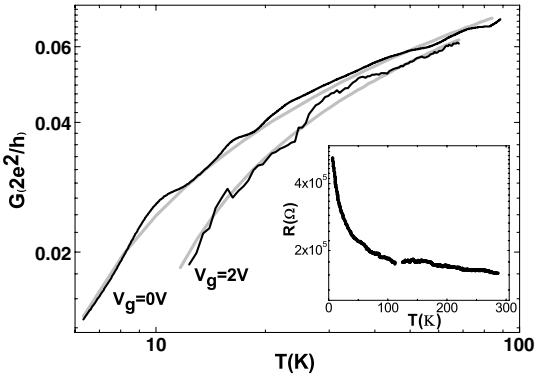

Figure 1. Conductance versus temperature for two gate voltage values, 0 and +2 V. Grey lines are theoretical curves following the WL model (see text). Inset, resistance versus temperature from 4 to 300 K.

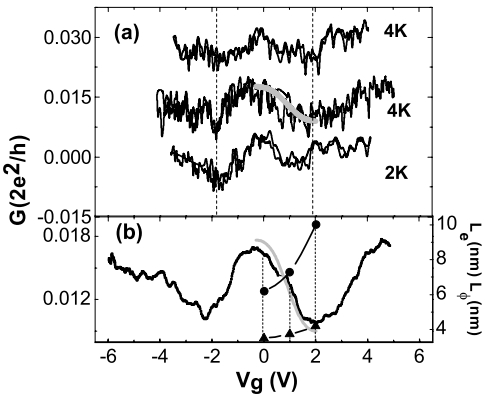

Figure 2. Differential conductance $\mathrm{d}I/\mathrm{d}V$ versus V_g at 4 and 2 K after different thermal cyclings. (a) Top curve shifted by $0.01G_0$, $\mathrm{d}I/\mathrm{d}V$ at 4 K and $V_\mathrm{bias} = 1$ mV. Middle curve, $\mathrm{d}I/\mathrm{d}V$ at 4 K and $V_\mathrm{bias} = 0.1$ mV and bottom curve shifted by $-0.015G_0$, $\mathrm{d}I/\mathrm{d}V$ at 2 K and $V_\mathrm{bias} = 0.1$ mV. The grey curve represents the fit of $G(V_\mathrm{g})$. (b) Smoothed $\mathrm{d}I/\mathrm{d}V$ measurements at 4 K. Black circles and triangles are respectively L_ϕ and l_e versus V_g and represent the gate voltage used for magnetoconductance measurement. The grey curve represents the fit of $G(V_\mathrm{g})$ (see the text).

in quantum interference appearance. It increases the electronic scattering probability on defects. By changing E_F, the energetic disorder configuration is displaced. As a consequence, conductance fluctuates as a function of V_g. For a hollow cylinder, UCFs are defined by $\Delta G = \sqrt{12}\frac{e^2}{h}(L_\varphi/L)^{3/2}$. The fluctuations of the order of 10^{-6} S that we measure at 4 K mean a coherence length equal to 10 nm, which is rather small. A smoothing of the UCF over several measurements clearly reveals the slow modulations of $G(V_\mathrm{g})$ (figure 2(b)). They are reproducible, robust to thermal cycling and persist up to 100 K (figure 1). As a consequence, charge effects can be ruled out.

Magnetoconductance $G(B)$ at 4 K (figure 3) is measured in parallel configuration $B_\parallel$ for different gate voltages as indicated in figure 2(b). The magnetoconductance is always positive and its magnitude strongly decreases with the zero field conductance. It reaches 83% at 30 T for the less conducting state under 2V. Along with UCF, an applied magnetic field induces WL suppression. For a hollow cylinder with a diameter $2R$ and a wall thickness $a = 0.14$ nm,

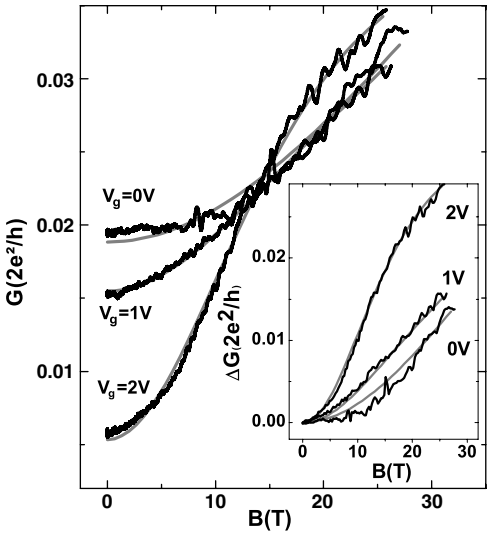

Figure 3. Conductance versus $B_{\parallel}$ at 4 K and for different gate voltages. Grey lines represent the theoretical curves of the conductance in the WL regime (see text). Inset, zoom on $\Delta G(B) = G(B) - G(0)$ for different $V_{\rm g}$ and the corresponding fits in grey lines using equation (1).

the magnetic field dependence of the WL contribution to the conduction is expressed by the Altshuler–Aronov–Spivak calculations [20]:

$$\Delta G_{\rm WL}(B) = -N\frac{e^2}{\pi\hbar}\frac{2\pi R}{L}\left[\ln\left(\frac{L_\varphi(B)}{L_\varphi}\right) + 2\sum_n\left(K_0\left(\frac{n2\pi R}{L_\varphi(B)}\right)\right.\right.$$
$$\left.\left.\times\ \cos\left(2\pi n\frac{2\phi}{\phi_0}\right) - K_0\left(\frac{n2\pi R}{L_\varphi}\right)\right)\right] \qquad (1)$$

where N is the number of channels, L is the length of the tube, $K_0(x)$ is the Macdonald function, $\Phi = \pi R^2 B$ and $\Phi_0 = h/e$. $L_\varphi(B)$ is the phase coherence length defined by $L_{\varphi(B)}^{-2} = L_\varphi^{-2} + (aeB/\hbar)^{2/3}$, where L_φ is the zero field phase coherence length in $B_{\parallel}$. We use two fitting parameters: the radius R and L_φ. N is *a priori* fixed to two (see below). Very convincing agreements are obtained between experimental $\Delta G(B)$ curves for several back-gate voltages and equation (1) (figure 3, inset). A unique radius value of $R = 3.5 \pm 0.1$ nm is obtained while L_φ is found to be significantly gate dependent: L_φ equals 7.2, 7.9 and 10.4 nm for $V_{\rm g}$ corresponding to 0, 1 and 2 V, respectively. The radius we infer matches reasonably well with the AFM observation and the L_φ estimates are comparable to the one deduced from the UCF analysis. Two remarks have to be made. First, although we reach $\Phi/\Phi_0 \approx 0.38$ at 30 T, we do not observe any hint of AB effects on the magnetoconductance. This is due to the L_φ and $l_{\rm e}$ lengths, which are well below the circumference of the tube. Second, equation (1) is usually multiplied by an extra parameter to account for non-transparent contacts in the two probe configuration [19]. In our case, attempts to use this parameter in the fitting process give a constant value very close to unity whatever the gate voltage is. This confirms the smallness of the resistance of contacts compared to the intrinsic tube resistance in our measurements. Even at 4 K, in the diffusive regime, most of the voltage drop occurs within the MWCNT.

In the WL regime, the CNT conductance is the sum of the classical part $G_{\rm cl}$ and the quantum correction $G_{\rm WL}$. $G_{\rm cl}$ is defined by $G_{\rm cl} = \frac{2e^2}{h}\frac{Nl_{\rm e}}{L}$. From the experimental zero field conductance values, we deduce an electronic mean path which is slightly gate voltage

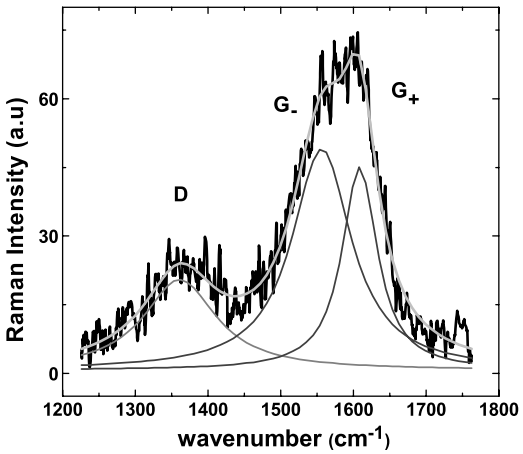

Figure 4. μ-Raman spectroscopy performed on the tube showing the three contributions of tangential phonon modes, the D, G_- and G_+ bands. The grey curves are Lorentzian fits.

dependent: l_e equals 5.15, 5.3 and 6.1 nm for V_g equal to 0, 1 and 2 V, respectively (grey lines in figure 3). Note that while the zero field conductance varies by a factor of four between 0 and 2 V, the $G(B)$ curves for different gate voltages merge to very close values above few tens of tesla once most of the WL contribution is suppressed. This gives evidence that the zero field value of the conductance and its energy dependence are dominated by the WL. Using the extracted values of L_φ and l_e versus V_g in equation (1), we found that the calculated $G(V_g)$ curve matches the data reasonably well (grey lines in figure 2).

Our interpretation in terms of WL is confirmed by the analysis of the temperature dependence of the conductance $G(T)$. Assuming that electron–electron interaction [21] is the mean source of phase coherence loss versus temperature, L_φ is therefore expressed by $L_\varphi = (\frac{DG_{cl}Lh^2}{2e^2kT})^{\frac{1}{3}} = AT^{-\frac{1}{3}}$ with $D = v_F l_e/2$ the diffusion coefficient and v_F the Fermi velocity. Replacing L_φ in equation (1) by its temperature dependence, we model the total conductance of the tube $G(T)$ for different electrostatic dopings (figure 1, grey lines), where A is the only unknown parameter. Convincing agreements are obtained for A equal to 1.3 and 1.94 nm $K^{1/3}$ under 0 and 2 V. This corresponds to L_φ values at 4 K ranging from 8 and 12 nm, in full agreement with the magneto-conductance analysis. Note that v_F can also be deduced since A and l_e are known: we find $v_F = 4 \times 10^3$ m s^{-1}, which is two orders of magnitude smaller than the theoretical value for a pristine tube.

2.2. Raman spectroscopy

The transport characteristic lengths depicted in figure 2(b) and the Fermi velocity we infer are rather small compared to other studies [19, 9, 7]. But they are strongly structural quality dependent. To probe the structural properties, we performed the μ-Raman spectroscopy on the *same* MWNT after the electronic transport measurements. Resonant Raman spectra are recorded in the back-scattering geometry, with a triple grating system (DILOR XY800) equipped with a cryogenic CCD detector with a spectral resolution of 1 cm^{-1}. The 545 nm line of an Ar^+ laser is focused on the sample with a 100× objective. The phonon frequencies are obtained by fitting the experimental peaks with Lorentzian functions (figure 4). The spectrum reveals the contribution of three tangential phonon modes. The first, the D band originating from a double resonant process induced by disorder, is at 1361 cm^{-1}. The second, G_-, band is

located at 1556 cm^{-1} and the last one, G_+, at 1608 cm^{-1}. The roughly equivalent intensities of G_- and G_+ imply that the MWCNT is mostly metallic [22]. The large magnitude of the D band is synonymous with defects [22]. The line widths of G_- and G_+, respectively 99 and 58 cm^{-1}, which have to be compared with the line width of pristine nanotubes, around 10 cm^{-1}, also support a strong disorder in our samples [23], the line width being inversely proportional to the phonon lifetime. This unambiguously confirms the predominance of structural defects, in agreement with the small values of L_φ, l_e and v_F.

3. Discussion

Our analysis of the magnetoconductance indicates that transport characteristic lengths depend on the location of the Fermi level. Of fundamental interest is the physical origin of the energy dependence of l_e and L_φ and the resulting modulations of the conductance. Simulations made in a coherent regime (with no energy dependence of L_φ) predict that defects (topological or impurity) cause conductance modulation in CNTs due to the energy dependent mean free path [12, 13]. A disordered metallic CNT exhibits a conductance drop near the vHs and in the vicinity of the scattering energy, which yields to the so-called resonant scattering [11]. Recent transport experiments [9] in the diffusive regime give evidence that the presence of vHSs modulates the conductance. In our case, we have assumed two conducting channels ($N = 2$) to extract the l_e and L_φ values. So we implicitly assume a Fermi energy location in the metallic bands. In fact, for an 8 nm diameter nanotube, the first vHSs are roughly separated by 300 meV. The shift of E_F as a function of V_g is defined by $\Delta E_F = e\frac{C_g}{C_{NT}}V_g$, with C_g the back-gate capacitance and C_{NT} the electrochemical capacitance of the tube expressed by $C_{NT} = e^2.DoS(E_F)$. Reaching the first vHS under 2 V bias would require an unrealistic gate capacitance of $7aF$, more than ten times larger than the maximum theoretical gate capacitance assuming a plane coupling with $C_g = \frac{\varepsilon_{SiO_2}S}{d}$ (ε_{SiO_2} is the SiO_2 dielectric constant, d its thickness and S the tube surface). Beside, a large shift of E_F far from the CNP is unlikely: low temperature experiments are performed under vacuum or He atmosphere and we are used from experiment to a change from a p-doped to an almost un-doped nanotube under these conditions. Therefore, it is unlikely that the conductance modulations we measure originate from entering into the vHS. We also point out that invoking a larger N ($N = 6$ in the first massive bands) provides unrealistic values in the order of nanometres, with L_φ becoming inferior to l_e. These arguments support the idea that disorder on the metallic band yields energy dependent l_e and L_φ lengths and controls the conductance modulations. Interestingly, l_e and L_φ vary in the same way: a slight decrease of l_e close to 0 V is related to a large decrease of L_φ and *increase* of the conductance. This experimental fact contradicts the existing conductance calculations versus energy [12, 13] where the conductance increases with increasing l_e. We clearly demonstrate that, in a disordered tube, L_φ is strongly energy dependent. As a consequence, the WL modulation dominates the classical part of the conductance. The conductance is therefore mainly driven by the modulation of L_φ instead of the modulation of l_e. When the WL contribution is destroyed by high magnetic fields, the standard behaviour of the conductance is recovered (figure 3): the highest conductance curve corresponds to the largest l_e.

4. Conclusion

We provide experimental evidence that, in the diffusive regime, the conductance is dominated by a large WL contribution. Its modulation versus energy is attributed to the energy dependence of L_φ in the presence of disorder. Recently, theoretical works [24] predicted that the electron–

phonon coupling may also induce some energy dependence of L_φ, assuming clean nanotubes. Our work should stimulate further theoretical works including electron–electron interactions for better understanding of the energy dependence of the characteristic lengths in disordered CNTs.

Acknowledgments

We are very thankful to Ph Lambin and the Nanocyl company for providing MWCNTs and E Flahaut for experimental assistance in MWCNT preparation and TEM observations. We gratefully acknowledge S Roche and F Triozon for stimulating discussions. Substrate preparations have been performed in the LAAS technological platform. This work has been supported by the French ministry of research under ACI programme 'Nanosciences 2004' No NR044 (NOCIEL) and by EuroMagNet under EU contract RII3-CT-2004-506239 of the Sixth Framework 'Structuring the European research area, research infrastructure actions'.

References

[1] Liang W, Bockrath M, Bozovic D, Hafner J H, Tinkham M and Park H 2001 *Nature* **411** 665
[2] Bockrath M, Cobden D H, Lu J, Rinzler A G, Smalley R E, Balents L and McEuen P L 1999 *Nature* **397** 598
[3] Tans S J, Devoret M H, Groeneveld R J A and Dekker C 1998 *Nature* **394** 761
[4] Bockrath M, Liang W, Bozovic D, Hafner J H, Lieber C M, Tinkham M and Park H 2001 *Science* **291** 283
[5] Frank S, Poncharal P, Wang Z L and deHeer W A 1998 *Science* **280** 1744
[6] Kanda A, Tsukagoshi K, Aoyagi Y and Ootuka Y 2004 *Phys. Rev. Lett.* **92** 036801
[7] Shonenberger C, Bachtold A, Strunk C, Salvetat J-P and Forro L 1999 *Appl. Phys.* A **69** 283
[8] Bachtold A, Strunk C, Salvetat J P, Bonard J M, Forro L, Nussbaumer T and Shonenberger C 1999 *Nature* **397** 673
[9] Stojetz B, Miko C, Forro L and Strunk C 2005 *Phys. Rev. Lett.* **94** 186802
[10] Ando T 2000 *Semicond. Sci. Technol.* **15** R13
[11] Choi H J, Ihm J, Louie S G and Cohen M L 2000 *Phys. Rev. Lett.* **84** 2917
[12] Triozon F, Roche S, Rubio A and Mayou D 2004 *Phys. Rev.* B **69** 121410
[13] Latil S, Roche S, Mayou D and Charlier J C 2004 *Phys. Rev. Lett.* **92** 256805
[14] Gomez-Navarro C, De Pablo P J, Gomez-Herrero J, Biel B, Garcia-Vidal F J, Rubio A and Flores F 2005 Tuning the conductance of single-walled carbon nanotubes by irradiation in the anderson localisation regime *Nat. Mater.* **4** 534
[15] Collins P G and Avouris Ph 2002 *Appl. Phys.* A **74** 329
[16] Javey A, Guo J, Wang Q, Lundstrom M and Dai H 2003 *Nature* **424** 654
[17] Sagnes M, Raquet B, Lassagne B, Broto J M, Flahaut E, Laurent Ch, Ondarçuhu Th, Carcenac F and Vieu Ch 2003 *Chem. Phys. Lett.* **372** 733
[18] Roche S and Saito R 2001 *Phys. Rev. Lett.* **87** 246803
[19] Fedorov G, Lassagne B, Sagnes M, Raquet B, Broto J M, Triozon F, Roche S and Flahaut E 2005 *Phys. Rev. Lett.* **94** 066801
[20] Aronov A G and Sharvin Y V 1987 *Rev. Mod. Phys.* **59** 755
[21] Altshuler B L, Aronov A G and Khmelnitsky D E 1981 *Solid State Commun.* **39** 619
[22] Dresselhaus M S, Dresselhaus G, Jorio A, Souza Filho A G and Saito R 2002 *Carbon* **40** 2043
[23] Jorio A, Fantini C, Dantas M S S, Pimenta M A, Souza Filho A G, Samsonidze Ge G, Brar V W, Dresselhaus G, Dresselhaus M S, Swan A K, Ünlü M S, Goldberg B B and Saito R 2002 *Phys. Rev.* B **66** 115411
[24] Roche S, Jiang J, Triozon F and Saito R 2005 *Phys. Rev. Lett.* **95** 076803